Biophys. Struct. Mechanism 4, 97–110 (1978)

Biophysics of Structure and Mechanism

Fluorescence Polarization of Stretched Polytene Chromosomes Stained with Acridine Orange

A. D. Gruzdev and G. P. Kishchenko

Institute of Cytology and Genetics, Siberian Branch of the USSR Academy of Sciences, Novosibirsk, USSR

Abstract. The molecules of the fluorescent dye acridine orange (AO) bind to DNA in such a way that the absorption and emission dipoles lie on a plane perpendicular to the DNA axis. For this reason, definite fluorescence polarization should correspond to each mode of spatial DNA packing. A chromosome, considered as an axially symmetrical ensemble of DNA, was characterized by two experimental parameters, $P_{\parallel}$ and $P_{\perp}$, i.e., by polarizations of fluorescence excited by light polarized parallel and perpendicular to the symmetry axis. In view of the sequential order in the packing levels of DNA fiber in a chromosome, it was suggested that, under mechanical stretching, the highest level is disrupted first, then the others, in the order of their sequence.

Isolated chromosomes of *Chironomus thummi* were stained with AO and stretched with needles of a micromanipulator. From the changes of $P_{\parallel}$ and $P_{\perp}$ measured during stretching it was concluded the polytene chromosome bands have three, at least, DNA packing levels, tentatively described as 100 Å fiber, 250 Å coil and chromomere.

Key words: Chromosomes – Acridine orange – Fluorescence polarization.

Introduction

The complex packing of DNA molecules in a chromosome may be subdivided into several hierarchical levels. X-ray and electron microscopy studies have suggested that the first level is a supercoil with average diameter about 100 Å and pitch 45 Å (Bram and Ris, 1971) or 120 Å (Pardon et al., Richards and Pardon, 1970). However, in view of the subunit structure of DNP fiber (Olins and Olins, 1974), it seems more likely that helix pitch is irregular.

According to Ris and Kubai (1970), 100 Å fibers are basic morphological units of a chromosome, whereas thicker fibers, frequently observed in the electron microscope, are artifacts. Having thoroughly analysed current fixation techniques, Chentsov and Poliakov (1974) came to the conclusion that thick, 200–250 Å fibers are naturally occurring structures.

0340-1057/78/0004/0097/$ 02.80

The finding of thicker fibers, about 500 Å in diameter, by electron microscopists (Du Praw and Bahr, 1969; Bahr, 1970; Tanaka and Jino, 1973) does not exclude their formation from thinner 200 Å fibers. Pooley et al. (1974) consider, and with good reason, that electron microscopy serves to little useful purposes in determining the real size of chromosome fibers.

The existence of a higher-chromomere-level of packing raises no doubts, because chromomeres are clearly seen at mitosis and meiosis, they form bands of polytene chromosome and can even be isolated from interphase nuclei (Sonnenbichler, 1969). However, whether all these structures are identical remains an open question.

Finally, the structure of metaphase chromosomes is characterized by a higher level of complexity (Chentsov and Poliakov, 1974).

A newly developed method was used to determine the number of packing levels in polytene chromosome bands. This method is independent of any of the so far described models. It is based in the assumption that stretching of a chromosome disrupts the highest level of DNA packing first and then the other levels in the order of their sequence. Changes in DNA packing during chromosome stretching were recorded as changes of fluorescence polarization of acridine orange (AO) bound to chromosomal DNA. Obviously, such measurements provide data on band structure, because, bands contain the bulk of DNA (Beermann, 1972) and the fluorescence recorded is directly related to DNA content. This method is feasible owing to the specific mode of the binding of the AO molecules to DNA with the excitation and emission dipoles of the AO molecules lying in a plane perpendicular to the DNA axis (Lerman, 1963). As a result, each order of DNA packing corresponds to a definite dipole distribution and, accordingly, to a definite fluorescence polarization. Thus, it was expected that the pattern of changes in the fluorescence polarization of the AO-stained polytene chromosomes would permit to count the number of DNA packing levels in their bands.

Materials and Methods

Polytene chromosomes from the nuclei of the fourth instar larvae of *Chironomus thummi* were used. Glands were excised with thin needles under a binocular microscope. To isolate nuclei and chromosomes from the glands, a slight modification of the method of Robert (1971) was adopted. Several glands were soaked with 1% saponin (Merck, BRD) for 30–40 min in small glass chambers and pipetted. Isolated nuclei or chromosomes were then transferred into polarization microfluorimeter chambers and stained for 15 min in 1 mg/ml acridine orange solution. The dye was purified as described by Friefelder and Uretz (1966).

After removing the unbound dye by serial changes of the solution in the chambers, needles of a micromanipulator were inserted into both ends of a large chromosome. The chromosome was gradually stretched out till it either broke or tore off from the needle.

In all the experiments, the solution utilised consisted of 125 mM NaCl, 1 mM $CaCl_2$ in 0.02 M phosphate buffer, pH 6.3. Staining and stretching were done at room temperature, all the procedures were performed in the cold.

The polarization microfluorimeter differed from the device of MacInnes and Uretz (1966) in that plane-polarized light, not natural light excited fluorescence of the preparation. An Arens' prism (polarizer) was placed before the condenser (A = 0.4). The prism was set into one of the two fixed positions: in one position, the vector $\vec{E}$ of the exciting beam was parallel to the chromosome axis $0Z$; in the other position, it was perpendicular to it (axis $0X$). Depending on these positions, two values of polarization, $P_{\parallel}$ and $P_{\perp}$, were measured, defined as $P_{\parallel} = (I_{zz} - I_{zx})/(I_{zz} + I_{zx})$ and $P_{\perp} = (I_{xx} - I_{xz})/(I_{xx} + I_{xz})$. Here the first index denotes the polarization of the exciting beam and the second index refers to fluorescence polarization. To analyse polarization, an additional Arens' prism (analyser) was placed behind the objective of the microscope (40 x 0.75, water immersion). Theoretically, the spatial distribution of DNA in a chromosome was described by two parameters $\langle l_z^2 \rangle$ and $\langle l_z^4 \rangle$, representing the normalized average projections of the second and fourth powers of DNA length onto the chromosome axis $0Z$. In other words, $\langle l_z^2 \rangle = \langle \cos^2 \theta \rangle$ and $\langle l_z^4 \rangle = \langle \cos^4 \theta \rangle$, where θ is the angle between a small portion of DNA and the chromosome axis (Fig. 1). The relation between $\langle l_z^2 \rangle$, $\langle l_z^4 \rangle$ and between the $P_{\parallel}$ and $P_{\perp}$ measured is given by formulae (6, 6′) in the Appendix.

Fluorescence intensity was measured by a photomultipler tube (FEU-25, USSR) with glass filters ZHS-18 ($\lambda > 500$ nm) and SZS-10 (USSR) placed in front of it to diminish red fluorescence of the AO dimers on DNA and RNA.

The exciting light from an Hg-arc source (HBO-200, Osram) was modulated to diminish the undesirable long-lived fluorescence of the lenses and passed through 4 cm of $CuSO_4$ solution (10 g $CuSO_4 \cdot 5\ H_2O$ in 100 ml H_2O) and a 4 mm glass filter (UFS-1, USS). To diminish the intensity of the exciting light reaching the photomultiplier, an adjustable slit was used as field aperture of a microscope which was imaged onto a chromosome.

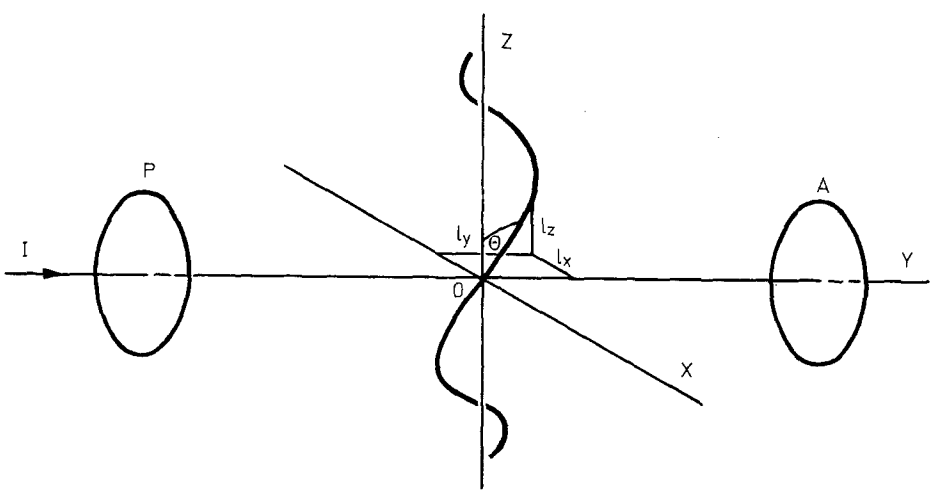

Fig. 1. A schematic diagram showing the direction of stretching of an acridine orange (AO) stained polytene chromosome of *Chironomus thummi* and the direction of light propagation along the axis $0Y$ of the optical system of the microfluorimeter. The polarizer P and the analyser A provide the orientation of the electric vector of the excited and emitted waves along the $0Z$ and $0X$ axis. A small portion of DNA molecules, near the origin of the coordinate makes an angle θ with the direction of stretching $0Z$

Results

Optimal conditions for chromosome staining were defined first. For this purpose, isolated nuclei and chromosomes were stained with AO of various concentrations. Figure 2 shows that with decreasing AO concentrations in the solution both degrees of fluorescence polarization tend asymptotically to $P_{\parallel} = P_{\perp} = 0.31$ and attain this value at an AO concentration of 1 μg/ml. Decrease in polarization at high AO concentrations has been attributed to an increase of the migration of excitation energy between DNA-bound molecules (Borisova et al., 1968). However, for the DNA-AO complex in the solution, the reported value of $P = 0.34$ (Borisova et al., 1968) exceeds the value $P = 0.31$ we obtained. This discrepancy was due to the high numerical aperture of the objective. Aperture effect was corrected when the experimental data were treated.

To test the specificity of AO-DNA binding and to evaluate the effect of AO binding to chromosomal protein, we attempted to quench AO-fluorescence with an external quencher (Korsunski and Naberukhin, 1972). Differences in fluorescence intensities between the AO-stained nuclei (or chromosomes) due to the replacement of NaCl by *KI* in the saline were measured. It was found that the external quencher produces no effect (error estimated within 2%). It was inferred that either the binding of AO to chromosomal protein was negligibly small or that these complexes occurred in a hydrophobic environment to which I^--ions had no access. Of these two assumptions, the former seemed more tenable, in view of the direct relation established between fluorescence intensity of AO in DNP and the number of free phosphate groups of DNA (Borisova and Minyat, 1970).

The last step was to express $P_{\parallel}$ and $P_{\perp}$ as functions of the length of the stretched chromosome. Typical recordings are presented in Figure 3a–c. The three pairs of curves follow a similar course. Each pair is antibatic, starts from a common point ($P_{\parallel} = P_{\perp} = 0.31$), passes through only one minimum and one maximum and has a long plateau. The previously stretched and relaxed chromosomes showed no such regularities. Their curves varied depending on the extent of the previous stretching which damaged irreversibly their structure (Fig. 3d).

Before discussing the results, it should be noted that averaging of the $P_{\parallel}$ and $P_{\perp}$ measured for various chromosomes and chromosome regions is out of question. In spite of their general resemblance, the curves for various chromosomes differ in

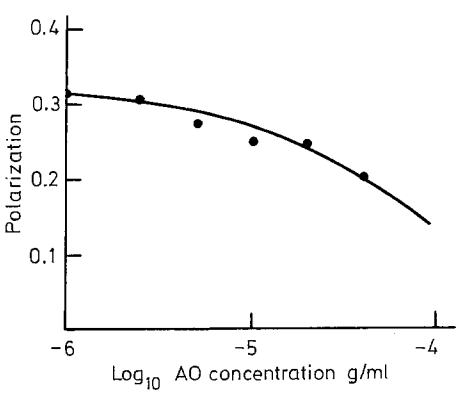

Fig. 2. Effect of the concentration of acridine orange (w/v) on the fluorescence polarization of the polytene chromosomes and nuclei of *Chironomus thummi*. $P_{\parallel}$ and $P_{\perp}$ coincide

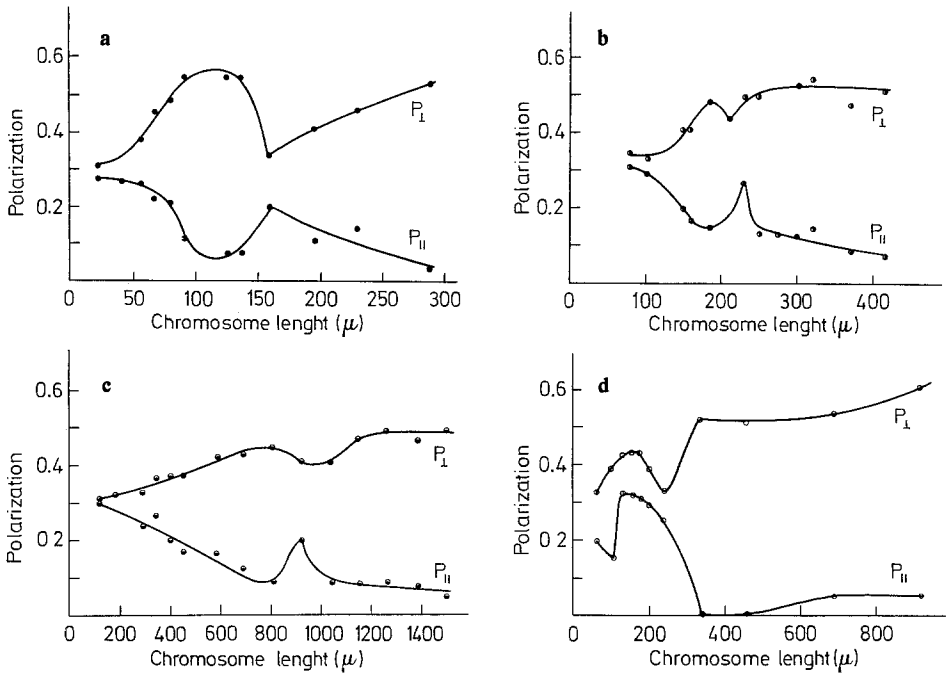

Fig. 3. Changes in the fluorescence polarization of polytene chromosomes during stretching. **a, b** and **c** — native chromosomes; **d** — a previously stretched and relaxed chromosome

significant details (in the abscissa scale, among other differences). This may be explained by two circumstances; the first was that unidentified sections of three large chromosomes (first, second and third) of *Ch. thummi* were measured and secondly, the distance between the needle tips was not the same from one experiment to another. Thus averaging of the data compared is possible only when DNA in the chromosomes is similarly oriented, not when the chromosomes are stretched to the same length or degree. With all these reservations, some conclusions, though qualitative, may be drawn from the experimental data.

Discussion

It is pertinent to recall that the experimental data concern band structure of polytene chromosomes, since bands contain the major bulk of chromosomal DNA and the light intensity recorded by the photomultiplier is proportional to the amount of DNA present.

The results made obvious some salient features of DNA packing in the bands of native unstretched chromosomes. It is apparent from Figure 3(a–c) that the starting points of $P_{\parallel}$ and $P_{\perp}$ coincide, i.e., fluorescence polarization does not depend on the direction of the vector $\vec{E}$ of the exciting light. This is possible only when DNA packing is spherically symmetrical. The spherical symmetry of DNA packing in the

bands of polytene chromosomes has been demonstrated earlier in fluorescence polarization (MacInnes and Uretz, 1966), and UV-dichroism studies (Wetzel et al., 1969). Data yielded by measuring polarization fluorescence do not permit to say definitely whether the spherically symmetrical mode of DNA packing is regular or entirely random. Moreover, it remains unclear, if a band consists of randomly lying anisotropic chromomeres or DNA is randomly distributed in a chromomere. We are prone to accept the latter possibility, because clear-cut anisotropy arises only at relatively high degrees of chromosome stretching (approximately fivefold), whereas very slight stretching may be sufficient to orient chromomeres.

Changes in the shape of the curves $P_{\parallel}$ and $P_{\perp}$ during chromosome stretching indicate the existence of two, at least, levels of DNA packing in bands. This is suggested by the unmonotonous relations between the two curves and the length of the stretched chromosome (Fig. 3). By contrast, an extended chromosome loses its morphological structure very monotonously, i.e., by blurring of band outlines and marked decrease of chromosome diameter. At slight degrees of stretching, fall of $P_{\parallel}$ and rise of $P_{\perp}$ indicate that the dipoles AO are mainly perpendicular to the chromosome axis. In the interval between the first and second extrema, some dipoles lie parallel to the chromosome axis. At the highest degree of stretching (beyond the second extrema), the dipoles reassume their perpendicular orientation with respect to the axis. DNA orientation in chromosomes is in strict conformance with the orientation of the AO dipoles. As a result of chromosome stretching, state III (randomly packed native DNA) is replaced by state II (DNA parallel to the chromosome axis), then follows state I (the part of DNA perpendicular to the axis) and, finally, DNA fiber (or a very similar packing state) appears.

The following considerations are developed in support of these assumed transitions. For each spatial DNA distribution in the chromosome structure, there is a definite value of the pairs $\langle l_z^2 \rangle$ and $\langle l_z^4 \rangle$ or a point on the plane $\langle l_z^2 \rangle$; $\langle l_z^4 \rangle$. Structural changes are always associated with changes in the position of the point.

The resulting curve (or phase trajectory) may be quite complex. For example, the deformation of a helix results in a parabola $\langle l_z^4 \rangle = \langle l_z^2 \rangle^2$. But in the case of the transition of structure A to B, the relation should be linear only. In fact, this case may be described by the set of equations:

$$\langle l_z^2(L) \rangle = C_A(L) \langle l_z^2 \rangle_A + C_B(L) \langle l_z^2 \rangle_B ;$$

$$\langle l_z^4(L) \rangle = C_A(L) \langle l_z^4 \rangle_A + C_B(L) \langle l_z^4 \rangle_B ;$$

$$C_A(L) + C_B(L) = 1 ,$$

where $C_A(L)$ and $C_B(L)$ are those portions of the structures which are changed during chromosome stretching. Having eliminated them, we obtain

$$\frac{\langle l_z^2(L) \rangle - \langle l_z^2 \rangle_A}{\langle l_z^4(L) \rangle - \langle l_z^4 \rangle_A} = \frac{\langle l_z^2 \rangle_B - \langle l_z^2 \rangle_A}{\langle l_z^4 \rangle_B - \langle l_z^4 \rangle_A}$$

i.e., the equation for the straight line passing through the coordinates of the first (A) and second (B) structures. The phase trajectory of Figure 3a–d is readily obtained from the formulae given in the Appendix. Figure 4a presents the relation between $\langle l_z^2 \rangle$ and $\langle l_z^4 \rangle$ for chromosome "a" (Fig. 3). The three straight lines correspond to the three transitions between the four states. The experimental points for all the

slightly stretched chromosomes (before the first extrema), whose original state was the same in all the cases, also lie on a straight line (Fig. 4b). By contrast, the relation between $\langle l_z^2 \rangle$ and $\langle l_z^4 \rangle$ for the previously stretched and relaxed chromosomes is very complex (Fig. 4c). No transition can be traced from one state to another.

Further interpretation of the experimental data calls for models of DNA packing, because DNA configuration cannot be determined solely from polarization fluorescence data. Clearly, the description of an elaborate configuration implies many parameters; however, only two measurable parameters are available.

As a rough approximation, we suggest a chromomere consisting of randomly packed fiber with DNA molecules arranged as a result of two successive coilings. Since the values $P_{\parallel}$ and $P_{\perp}$ for the random coil, the first order coil and the second order coil may be calculated from the formulae in the Appendix, it is quite conceivable how the values $P_{\parallel}$ and $P_{\perp}$ may change, when the model is stretched. All the possible variants of the transitions of the chromosome structure are schematically summarized in Figure 5: a) random coil → DNA fiber; b) random coil → first-order coil → DNA fiber; c) random coil → second-order coil → first-order coil → DNA

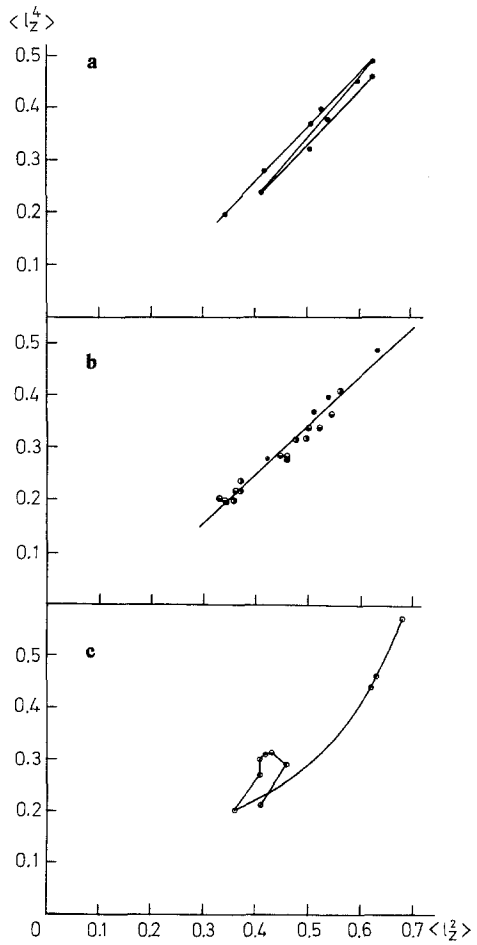

Fig. 4. Changes in parameters $\langle l_z^2 \rangle$ and $\langle l_z^4 \rangle$ of DNA packing during stretching of a polytene chromosome (phase trajectories). a) Phase trajectory of chromosome *a* (Fig. 3). The upper and lower point of the zigzag curve are the first and second extrema of *P*. b) Initial portions of the phase trajectories of three chromosomes *a, b, c* (Fig. 3) during stretching to the first extrema *P*. c) Phase trajectory of a previously stretched and relaxed chromosome *d* (Fig. 3)

fiber; d) random coil → second-order coil → DNA fiber. Obviously, the experimental curves (Fig. 3a–c) qualitatively agree only with item "c" of Figure 5 in which one minimum, one maximum and a long plateau are distinct.

The conformance between the packing ratios (the ratio of DNA length to chromosome length) measured directly and calculated for the model, confirms the validity of the model. In fact, DNA content in a haploid set of a laboratory stock of *Ch. thummi* has been found to be < 0.28 pg which corresponds to $85 \cdot 10^3$ μ of DNA length (Vlasova et al., 1976). The total length of a set of polytene chromosomes of this stock is 320 μ (Kiknadze and Gruzdev, 1970). In this case, the packing ratio is $K < 270$. For the model, however, $K = K_I K_2 K_c$, where K_I and K_2 are the packing ratios for the coils and K_c is that for the chromomere. For the DNP model of Pardon et al. (1967) $K_I = 2.8$ and for that of Bram and Ris (1971) $K_I = 4.3$. A tight coil with diameter of 250 Å composed of fiber 100 Å thick will have $K_2 = 8$. Finally, K_c can be calculated from the data of Figure 3. Evidently, complete orientation of the second-order coil can be achieved at chromosome extensions to the first extrema of P

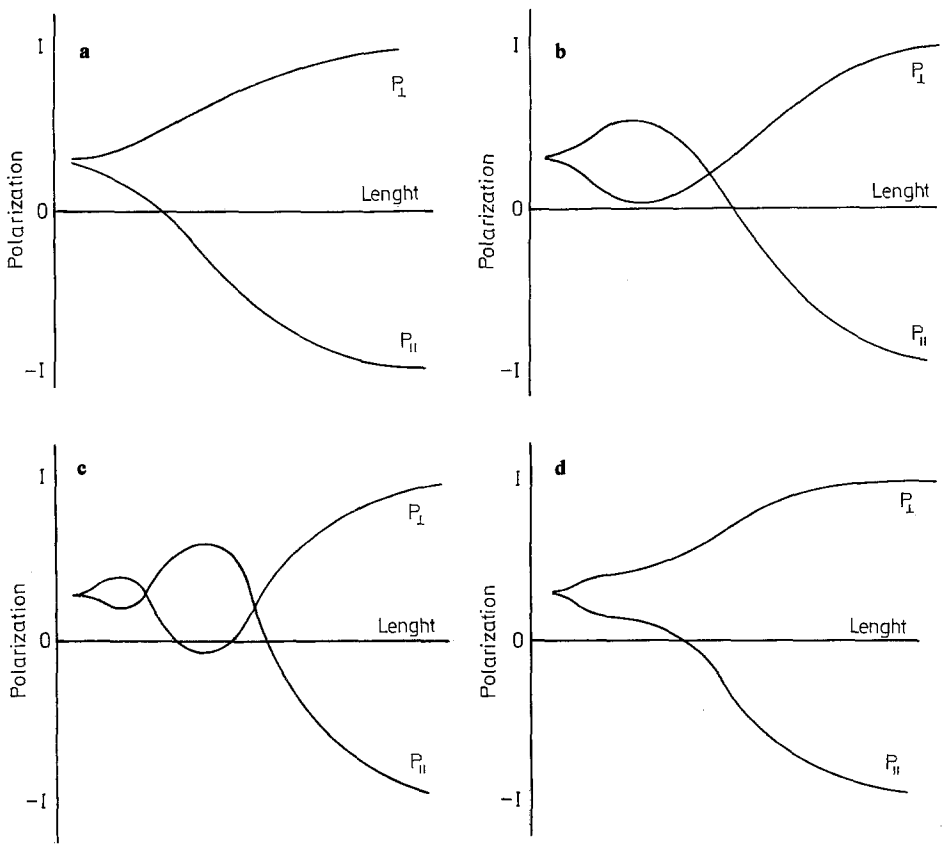

Fig. 5. A qualitative representation of changes in $P_\parallel$ and $P_\perp$ during stretching of a model chromomere undergoing the following transitions: a) random coil → DNA fiber; b) random coil → first-order coil → DNA fiber; c) random coil → second-order coil → first order coil → DNA fiber; d) random coil → second order coil → DNA fiber

or beyond them. Having compared the abscissae of the starting points of the curves and those of the peaks, we obtain $K_c > 5$. The total values of $K > 110$ (the model of Pardon et al., 1967) and $K > 170$ (the model of Bram and Ris, 1971) are close to the value we derived on the basis of measurements of DNA content and chromosome length.

The model's drawback is that the values of $P_{\parallel}$ and $P_{\perp}$ are significantly smaller (or larger, respectively) at the first extrema than the values calculated for the model. We believe that histon molecules prevent AO-binding to DNA segments of the coil that are aligned parallel to the chromosome axis. This might also be the cause of the seeming orientation of DNA along 80 Å fiber axis in the experiments of Dusenbury and Uretz (1972). The interpretation proposed may be too far-fetched to reflect faithfully the fiber structure of real chromosomes. We are hopeful that future refinements will insure a truer picture.

Appendix

Structure of an axially symmetrical ensemble of DNA molecules and its fluorescence polarization.

1. General Assumptions

Let a chromosome lie along $0Z$ in the plane $X0Z$ of a preparation. Then fluorescence polarizations are by definition:

$$P_{\parallel} = (I_{zz} - I_{zx})/(I_{zz} + I_{zx}); \quad P_{\parallel}\,(I_{xx} - I_{xz})/(I_{xx} + I_{xz})\,, \tag{1}$$

where I_{kl} are fluorescence intensities and the subscripts k, l correspond to the direction of the $\vec{\mathbf{E}}$ in the exciting (k) and the emitted (l) waves.

On the following assumptions, calculations of fluorescence intensities are applicable to any axially symmetrical ensembles of AO-stained DNA molecules.

1) Both dipoles of excitation and emission of DNA-bound molecules lie in a plane perpendicular to the DNA axis.

2) The AO-molecules are incoherent emitters.

3) There is no migration of excitation energy between the AO-molecules.

4) The AO-molecules have equal probabilities of binding to any base pair along a DNA molecule.

5) A chromosome is an axially symmetrical ensemble of DNA molecules.

Assumption 1) stems from the fact that the dipoles of the excitation and emission of π-electrons lie on the plane perpendicular to the DNA axis. This has been first observed by Lerman (1963) and proved later (Powers and Peticolos, 1967; Takesada et al., 1970).

Assumption 2) raises no doubt, if one takes into account that the dephasing collisions leading to the thermal relaxation of the excited state exert their effect rapidly (within 10^{-12} s), as compared to the fluorescence decay time (approximately 10^{-9} s).

Assumption 3) is valid only at low dye/phosphate ratios. High ratios produce fluorescence depolarization (Borisova et al., 1968). For this reason, we tested the adequacy of chromosome staining in preliminary experiments.

Assumption 4) raises strong objections, because histones definitely reduce dye binding to DNA (Borisova and Minyat, 1970). At present, however, it is unclear how histones are spatially distributed on DNA. Their effect can be calculated only after experimental and theoretical data have been compared.

Assumption 5) simply implies that there is no lateral asymmetry of DNA in a chromosome.

2. Fluorescence of a Small DNA Segment

Light flux dI into a solid angle $d\Omega$ from a dye molecule is proportional to: $(\vec{\mathbf{E}}'\,\vec{\mathbf{d}}')^2\,(\vec{\mathbf{E}}\,\vec{\mathbf{d}})^2$ or

$$\frac{dI_{e'e}}{d\Omega} = (\vec{\mathbf{e}}'\,\vec{\mathbf{d}}')^2(\vec{\mathbf{e}}\,\vec{\mathbf{d}})^2 \tag{2}$$

where $\vec{\mathbf{d}}'$ and $\vec{\mathbf{d}}$ are the dipoles of excitation and emission, respectively, and $\vec{\mathbf{E}}' = E'\vec{\mathbf{e}}'$ and $\vec{\mathbf{E}} = E\vec{\mathbf{e}}$ are the electric vectors of the exciting and emitted waves.

Let α be the angle between the dipoles $\vec{\mathbf{d}}'$ and $\vec{\mathbf{d}}$ and $\vec{\mathbf{l}}$ be the unit vector along the axis of the DNA molecule. Let the vectors $\vec{\mathbf{l}}$ and $\vec{\mathbf{e}}'$ be on the plane of the drawing (Fig. 6). Then $\vec{\mathbf{d}}'$ and $\vec{\mathbf{d}}$ will lie on the plane perpendicular to $\vec{\mathbf{l}}$. The angles given in Figure 6 may be introduced into formula (2) which is now written as:

$$\frac{dI_{e'e}}{d\Omega} = [\sin\varphi'\cos\theta]^2\,[\sin\varphi\cos(\beta - \alpha - \theta)]^2\,.$$

To calculate the light flux from a set N of AO-molecules bound to a small DNA segment, the previous formula has to be averaged for equally probable $+\alpha$ and $-\alpha$ and for the θ in the interval $0 \leqslant \theta \leqslant 2\pi$. After averaging, it assumes the form

$$\frac{dI_{e'e}}{d\Omega} = \frac{N}{4}\sin^2\varphi'\sin^2\varphi\,[(1 - \tfrac{1}{2}\cos 2\alpha) + \cos 2\alpha\cos^2\beta]$$

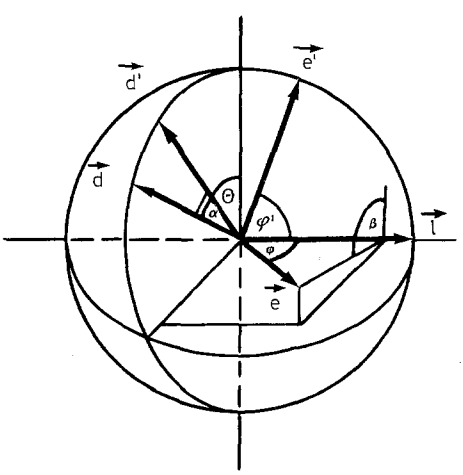

Fig. 6. Mutual direction of the electric vector of the exciting wave $\vec{\mathbf{e}}'$ and emitted wave $\vec{\mathbf{e}}$ and the absorption dipole $\vec{\mathbf{d}}'$ and emission dipole $\vec{\mathbf{d}}$ of an AO-molecule bound to a small segment $\vec{\mathbf{l}}$ of a DNA molecule

or the vector form

$$\frac{dI_{e'e}}{d\Omega} = \frac{N}{4}\left\{(1 - \tfrac{1}{2}\cos 2\alpha)\,[1 - (\vec{l}\,\vec{e}')^2]\,[1 - (\vec{l}\,\vec{e})^2] + \cos 2\alpha\,[(\vec{e}'\,\vec{e}) - (\vec{l}\,\vec{e}')\,(\vec{l}\,\vec{e})]\right\}. \tag{3}$$

3. Fluorescence of an Axially Symmetrical Ensemble of DNA Molecules

The axial symmetry of a chromosome (which, among other properties, means constancy of its fluorescence parameters during rotation around its axis) limits the number of measurable parameters of the spatial distribution of DNA molecules in a chromosome. When DNA distribution is entirely random, as in a solution, a single parameter is measured (e.g., polarization or fluorescence anisotropy). It is easy to see that an axially symmetrical system has two independent parameters.

To prove this, reduce formula (3) to

$$\frac{dI_{e'e}}{d\Omega} = N(l)\left[A^{(e'e)} + \sum_{k,l} B_{kl}^{(e'e)}\, l_k l_l + \sum_{k,l,m,n,} C_{klmn}^{(e'e)}\, l_k l_l l_m l_n\right], \tag{4}$$

where the subscripts k, l, m and n specify the orts of the rectangular coordinates. If there is an ensemble of DNA fibers or a single DNA molecule, spatially distributed in a complex manner, its fluorescence intensity may be written as

$$\frac{dI_{e'e}}{d\Omega} = N\left[A^{(e'e)} + \sum_{k,l} B_{kl}^{(e'e)}\,\langle l_k l_l\rangle + \sum_{k,l,m,n,} C_{klmn}^{(e'e)}\,\langle l_k l_l l_m l_n 7\right].$$

(Here the brackets $\langle\,\rangle$ indicate averaging over the ensemble.) Assuming that DNA distribution in a chromosome has cylindrical symmetry, it is easy to see that averaging eliminates all the members $\langle l_k l_l\rangle$ and $\langle l_k l_l l_m l_n\rangle$, except $\langle l_k^2\rangle$ and $\langle l_k^2 l_l^2\rangle$.

Furthermore, from cylindrical symmetry it follows that every $\langle l_k^2 l_l^2\rangle$ and $\langle l_k^2\rangle$ may be expressed as a linear combination of any two of them. If the pair $\langle l_z^2\rangle$ and $\langle l_z^4\rangle$ is chosen, simple calculations yield

$$\frac{dI_{e'e}}{d\Omega} = N\,(A^{(e'e)} + B^{(e'e)}\,\langle l_z^2\rangle + C^{(e'e)}\,\langle l_z^4\rangle), \tag{5}$$

where

$$A_{xx} = \tfrac{3}{8}(1 + \tfrac{1}{2}\cos 2\alpha); \quad A_{xz} = A_{zx} = \tfrac{1}{2}(1 - \tfrac{1}{2}\cos 2\alpha);$$
$$A_{zz} = 1 + \tfrac{1}{2}\cos 2\alpha;$$
$$B_{xx} = \tfrac{1}{4}(1 + \tfrac{1}{2}\cos 2\alpha); \quad B_{xz} = B_{zx} = \tfrac{1}{2}\cos 2\alpha;$$
$$B_{zz} = -2(1 + \tfrac{1}{2}\cos 2\alpha);$$
$$C_{xx} = \tfrac{3}{8}(1 + \tfrac{1}{2}\cos 2\alpha); \quad C_{xz} = C_{zx} = \bar{V}\,\tfrac{1}{2}(1 + \tfrac{1}{2}\cos 2\alpha);$$
$$C_{zz} = 1 + \tfrac{1}{2}\cos 2\alpha. \tag{5'}$$

From the formula it follows that there are only two parameters $\langle l_z^2\rangle$ and $\langle l_z^4\rangle$ at our disposal to characterize the complex DNA packing in a chromosome actually requiring many parameters for its description. Additional experimental data are

clearly needed to make measurement data of fluorescence intensity adequate for the building of a model of DNA distribution in a chromosome.

Parameters $\langle l_z^2 \rangle$ and $\langle l_z^4 \rangle$ may be calculated for simple models. Evidently, for a straight DNA segment $\langle l_z^2 \rangle = \langle l_z^4 \rangle = 1$. For randomly distributed DNA, $\langle l_z^2 \rangle = 1/3$, $\langle l_z^4 \rangle = 1/5$. For supercoiled DNA which makes a constant angle χ with the coil axis $\langle l_z^2 \rangle = \cos^2 \chi$, $\langle l_z^4 \rangle = \cos^4 \chi$. For second-order supercoil obtained from a first-order supercoil, calculations are not difficult, if coil deformation of the first-order supercoil may be regarded as negligible. For this purpose, the vector $\vec{l}$ of the first-order supercoil is decomposed into its components: $1 \cdot \cos\chi_1$, which is directed along the supercoil axis, and the component $l \cdot \sin\chi_1$, which is perpendicular to the axis. The sum of their projections onto the axis of the second-order supercoil gives l_z. After raising to the second and fourth power and averaging over a turn of the second-order coil, we obtain

$$\langle l_z^2 \rangle = \cos^2 \chi_1 \cos^2 \chi_2 + \tfrac{1}{2} \sin^2 \chi_1 \sin^2 \chi_2 ;$$

$$\langle l_z^4 \rangle = \langle l_z^2 \rangle^2 + \tfrac{1}{2} \sin^2 2\chi_1 \sin^2 2\chi_2 .$$

4. Aperture Effects

In formula (5), the exciting and emitted waves were considered to be flat. However, both the condenser and the objective of the microphotometer have final apertures, the effect of which results in an appreciable decrease in polarization P. Aperture effect may be taken into account as follows.

The spheric wave propagating along the axis $0Y$ may be regarded as a series of superimposed flat waves. Besides the component e_x (or e_z) of the electric vector, each flat wave has the component e_y. For this reason, the total intensity of the light falling on the objective of the microfluorimeter, when the analyser is oriented along the axis $0X$, is expressed as

$$I_{e'x} = (a_x \langle e_x^2 \rangle + a_y \langle e_y^2 \rangle)\, \Omega ,$$

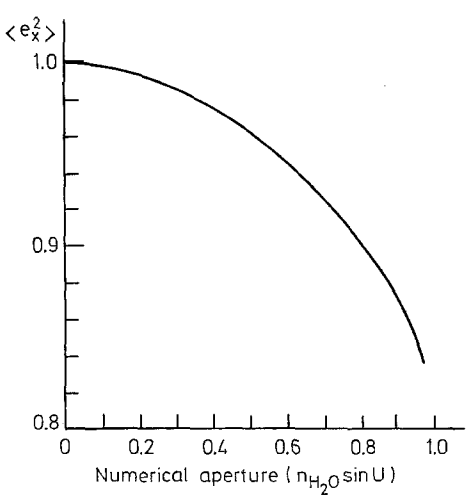

Fig. 7. Calculated dependence of $\langle l_x^2 \rangle$ on the objective aperture

where a_x and a_y are calculated from (3) and

$$\langle e_x^2 \rangle = \frac{1}{\Omega} \int e_x^2 \, d\Omega \; ; \quad \langle e_y^2 \rangle = \frac{1}{\Omega} \int e_y^2 \, d\Omega \; .$$

Because $\langle e_x^2 \rangle + \langle e_y^2 \rangle = 1$, it is sufficient to calculate only one of them. Computer calculations of $\langle e_x^2 \rangle$ for small condenser apertures are given in Figure 7. However, thanks to the reversibility of the light beams, Figure 7 may be also used to estimate condenser effect.

For the condenser we used in the microfluorimeter, $A = 0.4$, the exciting beam may be regarded as a flat wave with a small error of about 2%. For the objective with $A = 0.75$, we obtain $\langle e_x^2 \rangle = \langle e_z^2 \rangle = 0.91$ and $\langle e_y^2 \rangle = 0.09$.

Consequently, the total intensity of light falling on the objective of the microfluorimeter may be written as:

$$I_{kl} = A_{kl} + B_{kl} \langle l_z^2 \rangle + C_{kl} \langle l_z^4 \rangle \tag{6}$$

where

$$\begin{aligned} A_{xx} &= 0.35 + 0.18 \cos 2\alpha; \; A_{xz} = \; 0.47 - 0.22 \cos 2\alpha; \\ B_{xx} &= 0.29 + 0.06 \cos 2\alpha; \; B_{xz} = \; 0.07 + 0.39 \cos 2\alpha; \\ C_{xx} &= 0.35 + 0.18 \cos 2\alpha; \; C_{xz} = -0.44 - 0.22 \cos 2\alpha; \\ A_{zz} &= \; 0.95 + 0.43 \cos 2\alpha; \; A_{zx} = 0.50 - 0.25 \cos 2\alpha; \\ B_{zz} &= -1.82 - 0.86 \cos 2\alpha; \; B_{zx} = 0.50 \cos 2\alpha; \\ C_{zz} &= \; 0.86 + 0.43 \cos 2\alpha; \; C_{zx} = -0.5 - 0.25 \cos 2\alpha. \end{aligned} \tag{6'}$$

This is the final form for experimental data treatment.

We conclude that formulae (5), (6), and (1) make possible the calculation of fluorescence polarization for models with known spatial DNA distribution, i.e., with known $\langle l_z^2 \rangle$ and $\langle l_z^4 \rangle$; and, vice versa, the parameters of distribution, $\langle l_z^2 \rangle$ and $\langle l_z^4 \rangle$ may be derived from the experimental values $P_\parallel$ and $P_\perp$

Acknowledgements. The authors are indebted to Professor Yu. I. Naberukhin for critical analysis of the physico-mathematical framework. They also thank Professor I. I. Kiknadze and Dr. A. I. Sherudilo for discussions in the course of this work. Thanks are due to A. Fadeeva for translating this paper from Russian into English.

References

Bahr, G. F.: Human chromosome fibers. Considerations of DNA-protein packing and of looping patterns. Exp. Cell Res. **62**, 39–49 (1970)

Beermann, W.: Chromomeres and genes. In: Developmental studies on giant chromosomes (ed. W. Beermann). Berlin-Heidelberg-New York: Springer 1972

Borisova, O. F., Horachek, P., Gursky, G. V., Minyat, E. E., Tumanyan, V. G.: Energy transfer between dye molecules absorbed on DNA. Molec. Biol. (Russian) **2**, 475–488 (1968)

Borisova, O. F., Minyat, E. E.: Dissociation and distribution of histones in DNP. Molec. Biol. (Russian) **4**, 754–761 (1970)

Bram, S., Ris, H.: On the structure of nucleohistone. J. molec. Biol. **55**, 325–336 (1971)

Chentsov, Y. S., Poliakov, V. Y.: Ultrastructure of cell nucleus. Moscow: Nauka 1974. (Russian)

DuPraw, E. J., Bahr, G. F.: The arrangement of DNA in human chromosomes, as investigated by quantitative electron microscopy. Acta cytol. **13**, 188–205 (1969)

Dusenbury, D. B., Uretz, R. B.: The orientation of DNA within 80-Ångström chromatin fiber. J. cell. Biol. **52,** 639–648 (1972)

Friefelder, D., Uretz, R. B.: Mechanism of photoinactivation of coliphage T7 sensitized by acridine orange. Virology **30,** 97–103 (1966)

Kiknadze, I. I., Gruzdev, A. D.: Change in chromosome length related to polyteny in the chironomid salivary glands. Tsitologia (Russian) **12,** 953–960 (1970)

Kiknadze, I. I., Vlasova, I. E., Sherudilo, A. I.: Quantitative analysis of DNA content in the salivary gland chromosomes of *Chironomus thummi* at larval and prepupal stages. Tsitologia (Russian) **17,** 420–426 (1975)

Korsunsky, V. I., Naberukhin, Yu. I.: Fluorescence quenching of complexes of acridine dyes with nucleic acids. Molec. Biol. (Russian) **6,** 737–746 (1972)

Lerman, L. S.: The structure of the DNA-acridine complex. Proc. Nat. Acad. Sci. USA **49,** 94–102 (1963)

MacInnes, J. W., Uretz, R. B.: Organization of DNA in Dipterian polytene chromosomes as indicated by polarized fluorescence microscopy. Science **151,** 689–691 (1966)

Olins, A. L., Olins, D. E.: Spheroid chromatin units (ν-bodies). Science **183,** 330–332 (1974)

Pardon, J. F., Wilkins, M. H. F., Richards, B. M.: Super-helical model for nucleohistone. Nature (Lond.) **215,** 508–509 (1967)

Pooley, A. S., Pardon, J. F., Richards, B. M.: The relation between the unit thread of chromosomes in isolated nucleohistone. J. molec. Biol. **85,** 533–549 (1974)

Powers, J. C., Peticolas, W. L.: Kerr constant dispersion. III. The interaction of acridine orange with DNA. J. Phys. Chem. **71,** 3191–3195 (1967)

Richards, B. M., Pardon, J. F.: The molecular structure of nucleohistone. Exp. Cell Res. **62,** 184–196 (1970)

Ris, H., Kubai, D. F.: Chromosome structure. Ann. Rev. Genet. **4,** 263–294 (1970)

Robert, M. N.: Einfluß von Ionenstärke und pH auf die differentielle Dekondensation der Nukleoproteide isolierter Speicheldrüsen-Zellkerne und -Chromosomen von *Chironomus thummi.* (Lond.) Chromosoma **36,** 1–33 (1971)

Sonnenbichler, J.: Substructures of chromosomes. Nature (Lond.) **233,** 205–206 (1969)

Takesada, H., Saito, E., Fujita, H., Suzuki, K., Wada, A.: Study on the binding nature of acridine orange to DNA by means of flow dichroism. Bull. Chem. Soc. Japan **43,** 181–189 (1970)

Tanaka, K., Jino, A.: Demonstration of fibrous component in hepatic interphase nuclei by high resolution scanning electron microscopy. Exp. Cell Res. **81,** 40–46 (1973)

Wetzel, R., Buder, E., Schälike, W., Zirwer, D.: Linearer Dichroismus bei Riesenchromosomen von *Chironomus.* Chromosoma **26,** 201–20 (1969)

Received December 10, 1976/Accepted June 21, 1977